

This document is downloaded from DR-NTU, Nanyang Technological University Library, Singapore.

Title	Residual stress of high strength steel box T-joints Part 1 : experimental study
Author(s)	Lee, Chi King; Chiew, Sing Ping; Jiang, Jin
Citation	Lee, C. K., Chiew, S. P., & Jiang, J. (2014). Residual stress of high strength steel box T-joints. Journal of Constructional Steel Research, 93, 20-31.
Date	2013
URL	http://hdl.handle.net/10220/19806
Rights	© 2014 Elsevier Ltd. This is the author created version of a work that has been peer reviewed and accepted for publication by Journal of Constructional Steel Research, Elsevier Ltd. It incorporates referee's comments but changes resulting from the publishing process, such as copyediting, structural formatting, may not be reflected in this document. The published version is available at: [DOI: http://dx.doi.org/10.1016/j.jcsr.2013.10.003].

Table 1. Mechanical properties of HSS RQT701 plate at room and elevated temperatures.

Temperature	20	100	200	300	400	500	600	700	800
Young's modulus (GPa)	201.3	202.7	205.7	192.3	202.7	154.9	131.9	90.4	57.6
Yielding stress (MPa)	770	757	745	734	675	173	94	40	43
Ultimate stress (MPa)	909	871	847	865	727	428	171	99	66

Table 2. Welding parameters for box sections and T-joints.

Process	Electrode		Current		Volts (V)	Inter Pass Temperature (°C)
	Class	Diameter	Type	Amplitude (A)		
FCAW	E111T1-K3	1.2mm	DCEP	300-320	30-32	170-210

Table 3. Comparison of results with other studies

Study	*Yield strength or 0.2% proof stress (MPa)	*#Range of transverse residual stress (MPa)	&Normalized range of residual stress
Hot rolled and built up I-section [1]	Nominal: 415	Hot rolled: 0 to 70 Built up (welded): 340 to 400	Hot rolled: 0 to 17% Built up (welded): 80% to 96%
Mild steel (S355 J2 H) Tubular K-joint using [9]	Nominal: 355MPa Coupon minimum: 430 Coupon maximum: 630	250 to 400	Nominal: 70% to 100% (yield) Coupon minimum: 58% to 93% Coupon maximum: 40% to 64%
Q460 steel welded box section [10]	Nominal: 460 Coupon: 506	300 to 400	Nominal: 65% to 87% Coupon: 59% to 79%
This study, with preheating	Nominal: 690 Coupon: 770	Near corner: 100 to 350 Middle of brace: 10 to 120	Near corner, nominal: 15% to 50% Near corner, coupon: 13% to 45% Middle of brace, nominal: 1.5% to 17% Middle of brace, coupon: 1.2% to 16%
This study, without preheating	Nominal: 690 Coupon: 770	Near corner: 200 to 415 Middle of brace: 85 to 250	Near corner, nominal: 29% to 60% Near corner, coupon: 26% to 54% Middle of brace, nominal: 12% to 36% Middle of brace, coupon: 11% to 32%

* Values rounded to the nearest 1MPa.

Values measured by the hole drilling method within 10-15mm of weld toe.

& Values normalized with respect to yield strength or 0.2% proof stress, rounded to the nearest 1%.

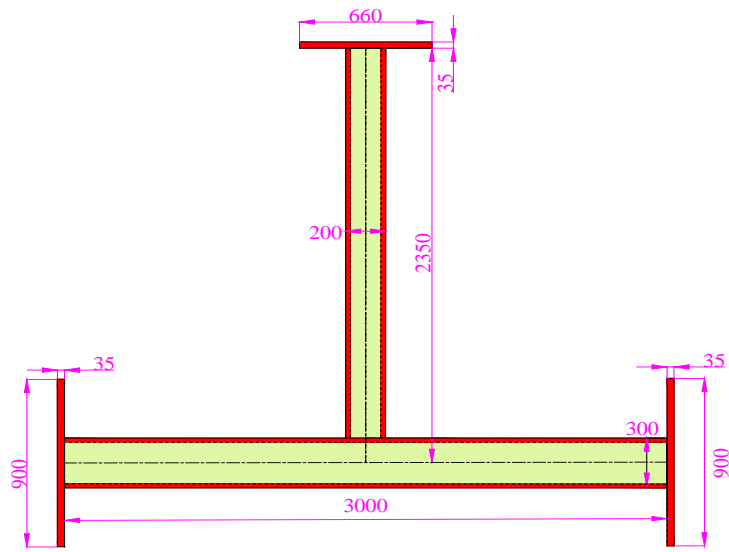


Fig. 1. Dimensions of the HSS box section T-joint.

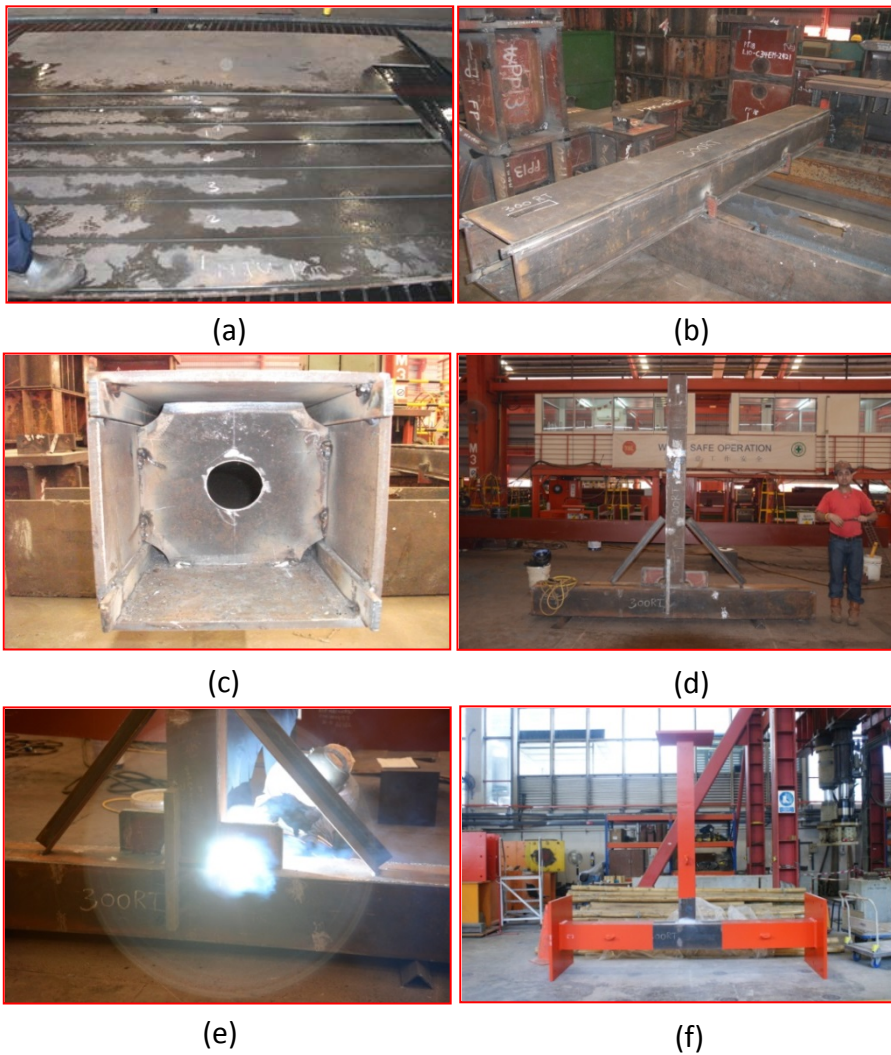


Fig. 2. Fabrication procedure of HSS box section T-joint.

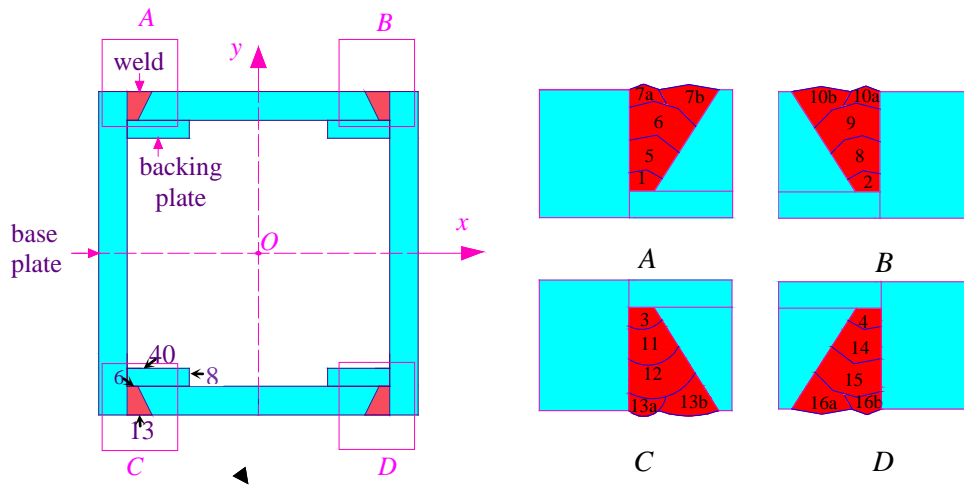


Fig. 3. The cross section and welding sequence of box sections.
(All dimensions in mm)

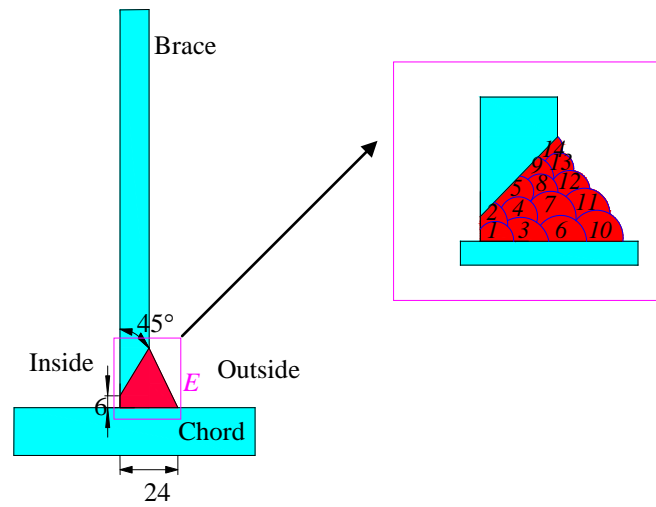
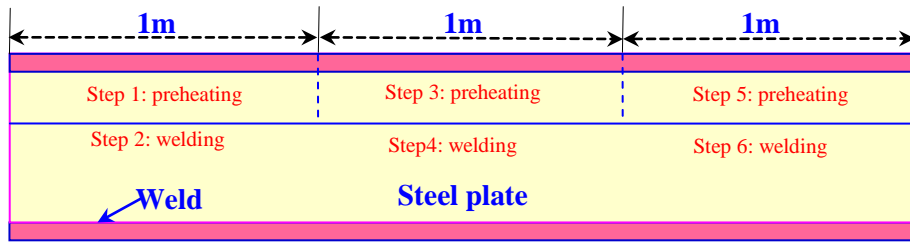


Fig. 4. Welding sequence of the HSS box section T-joint.
(All dimensions in mm)



(a) Preheating sequence in one weld pass in the box length direction



(b) Photo of fabricated box after welding

Fig. 5. Preheating and welding steps employed in the welding process of the box sections.

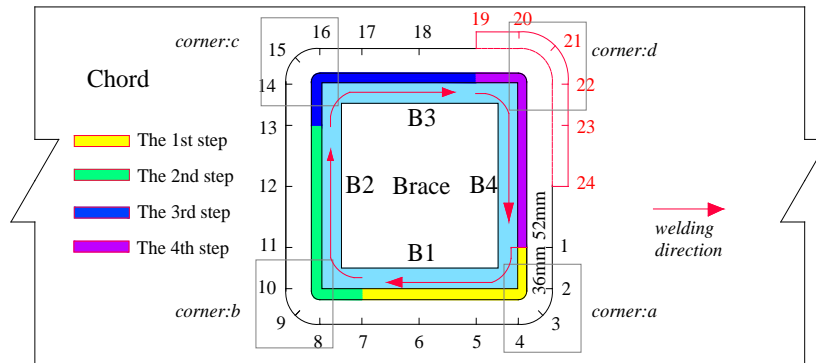


Fig. 6. Welding direction during joint fabrication.

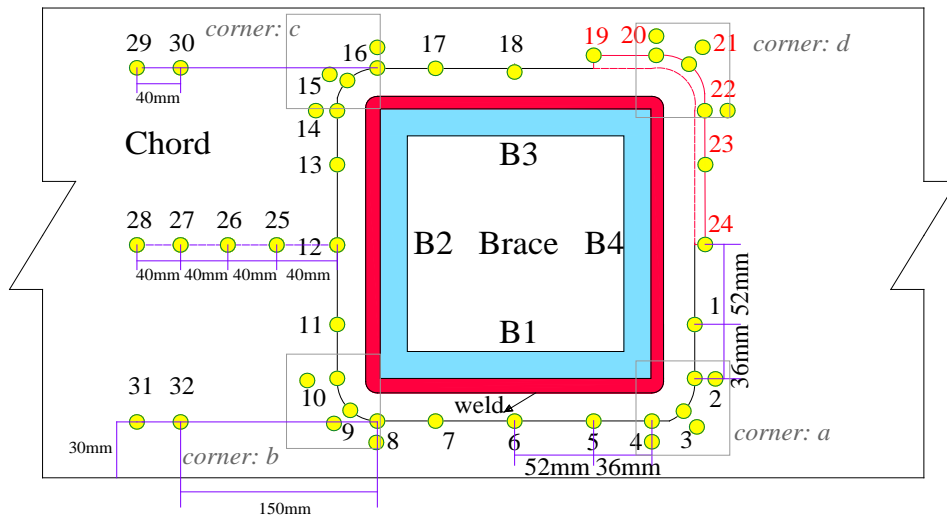


Fig. 7. Strain gauges pattern employed for the ambient temperature specimen.

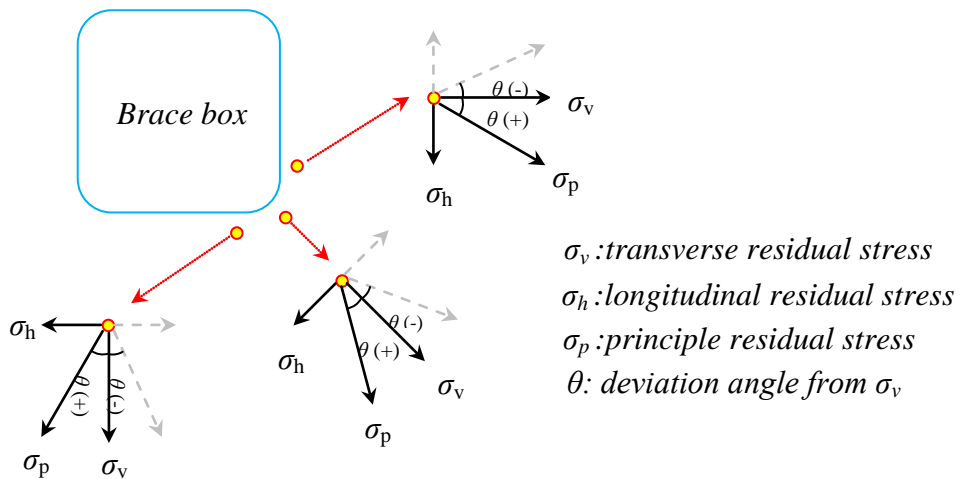


Fig. 8. Sign conventions for different residual stress components.

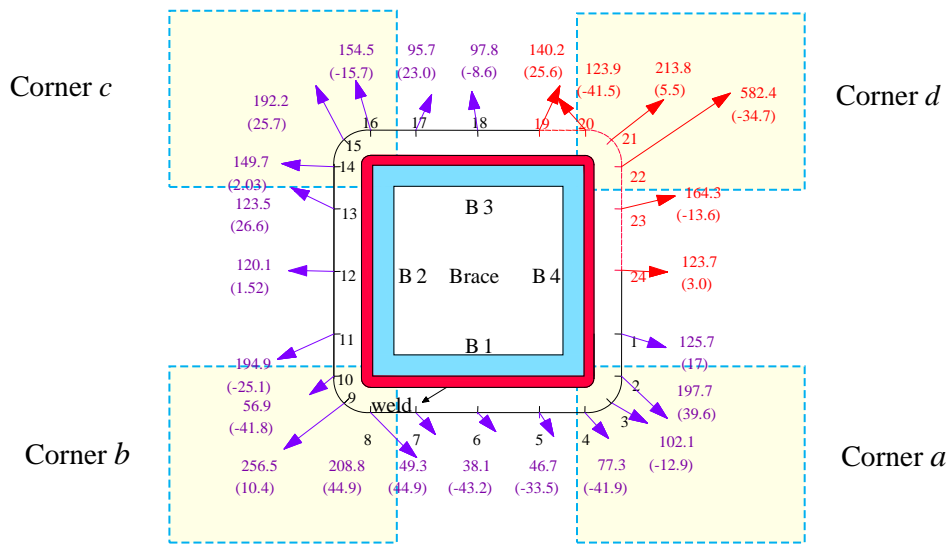


Fig. 9. Maximum principle stress distribution for the preheated specimen at positions 10/15mm from the chord weld toe.
(unit: MPa, values enclosed in brackets are θ in degree)

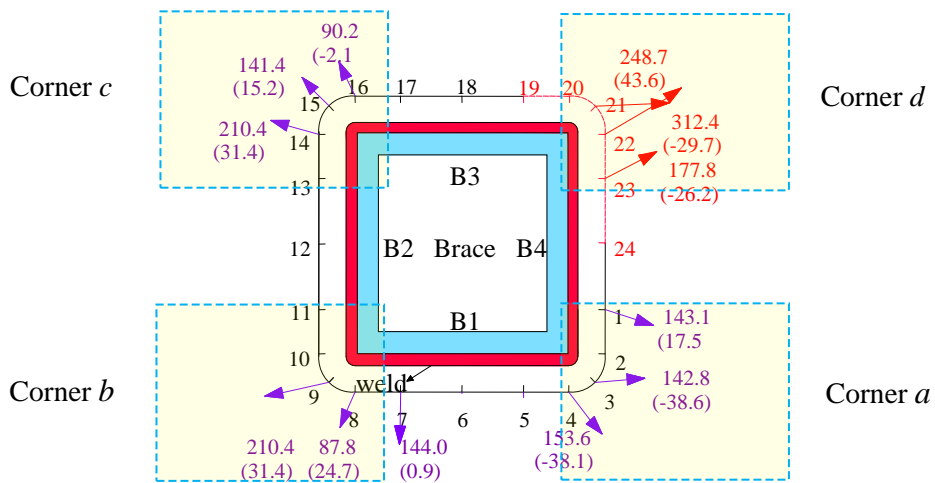


Fig. 10. Maximum principle stress distribution for the preheated specimen at positions 20/25mm from the chord weld toe at the four corners.
(unit: MPa, values enclosed in brackets are θ in degree).

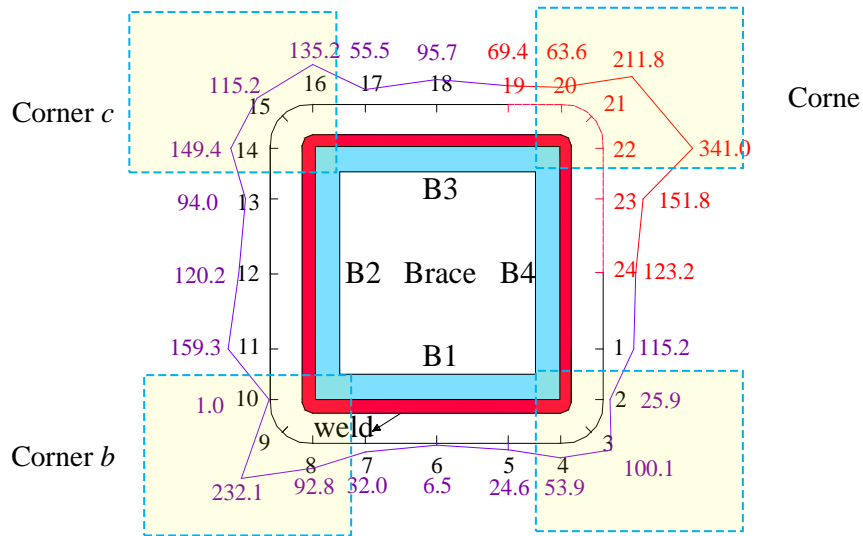


Fig. 11. Transverse residual stress distribution for the preheated specimen at positions 10/15mm from the chord weld toe.
(unit: MPa)

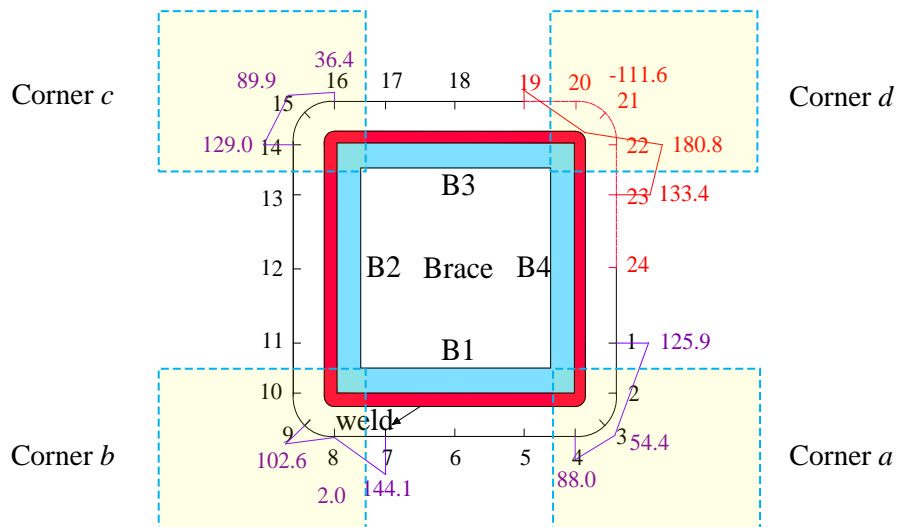


Fig. 12. Transverse residual stress distribution for the preheated specimen at positions 20/25mm from the chord weld toe at the four corners.
(unit: MPa)

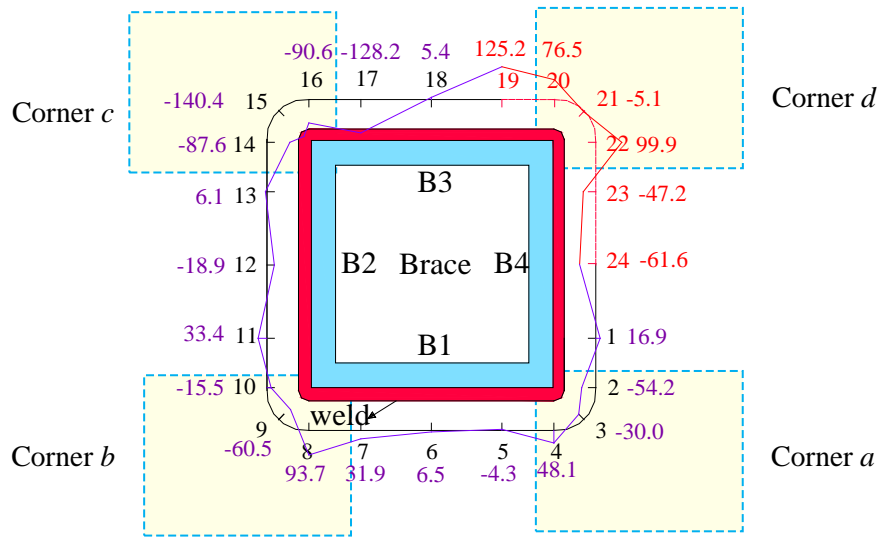


Fig. 13. Longitudinal residual stress distribution for the preheated specimen at positions 10/15mm from the chord weld toe.
(unit: MPa)

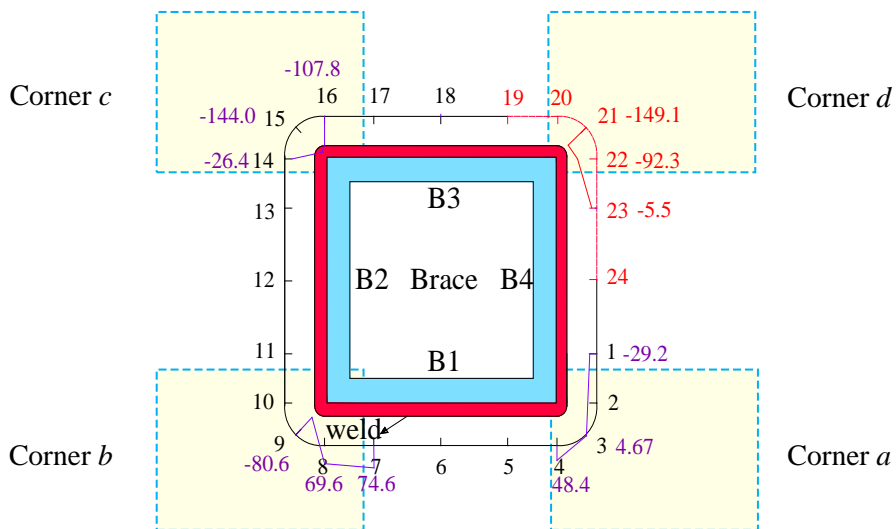


Fig. 14. Longitudinal residual stress distribution for the preheated specimen at positions 20/25mm from the chord weld toe at the four corners.
(unit: MPa)

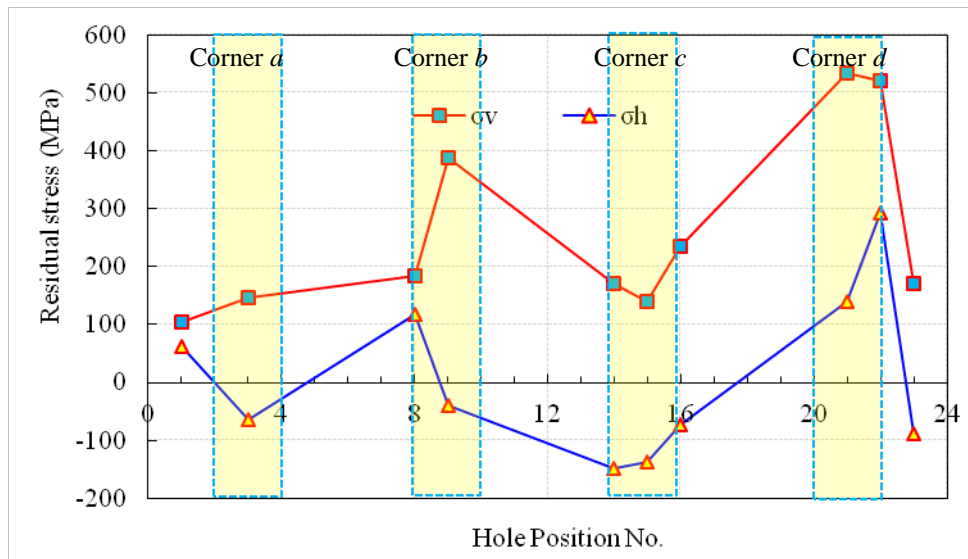


Fig. 15. Variations of transverse and longitudinal residual stresses at the chord weld toe estimated by linear interpolation for the preheated specimen.
 (σ_v : transverse stress, σ_h : longitudinal stress)

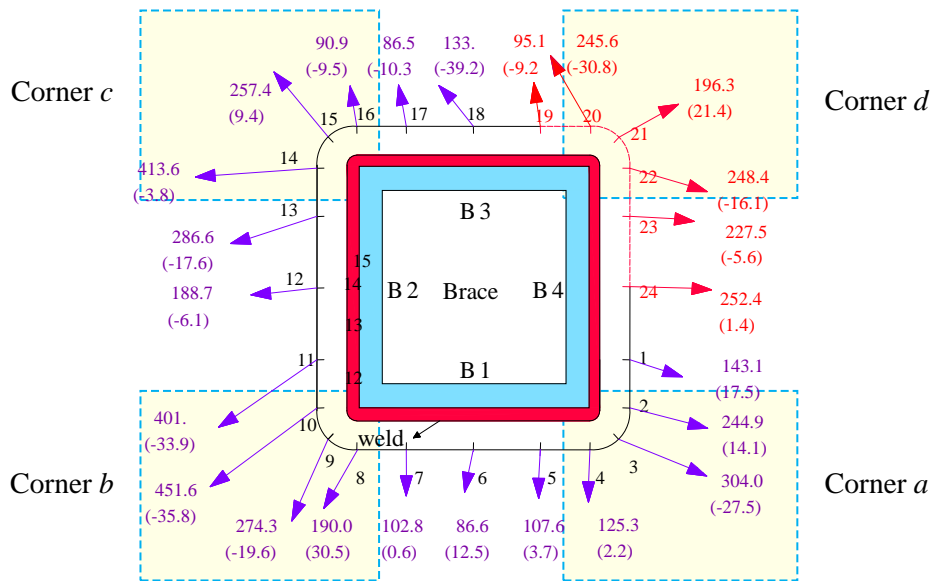


Fig. 16. Principle stress distribution for the ambient temperature specimen at positions 10/15mm from the chord weld toe.
(unit: MPa, values enclosed in brackets are θ in degree)

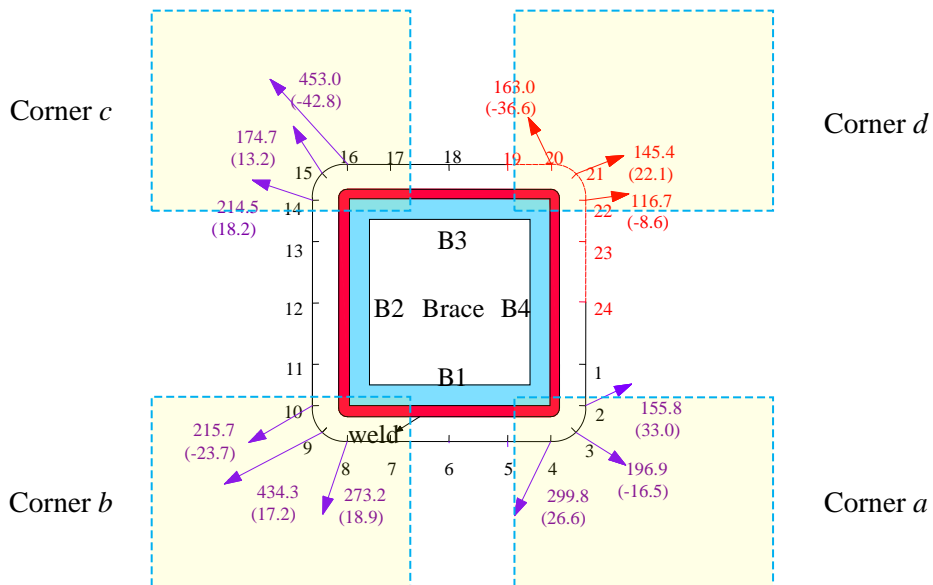


Fig. 17. Principle stress distribution for the ambient temperature specimen at positions 20/25mm from chord weld toe at the four corners.
(unit: MPa, values enclosed in brackets are θ in degree)

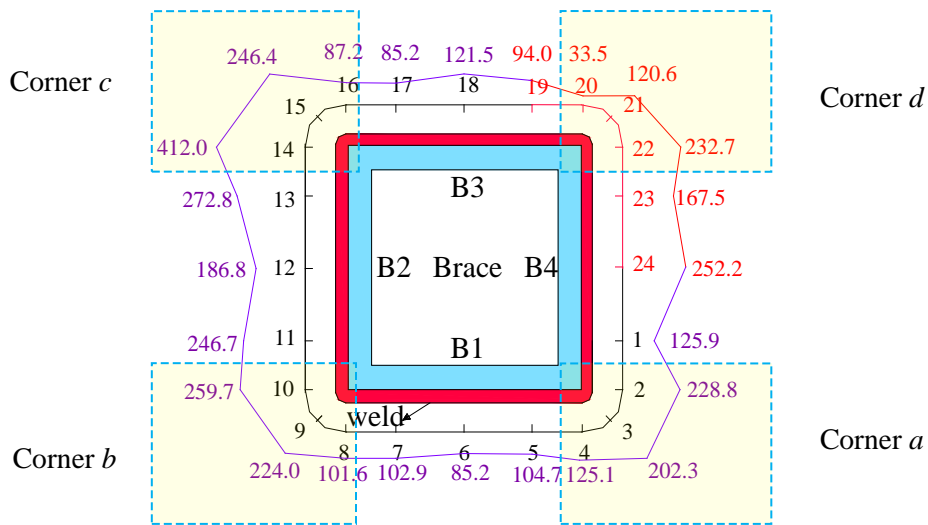


Fig. 18. Transverse residual stress distribution for the ambient temperature specimen at positions 10/15mm from the weld toe.
(unit: MPa)

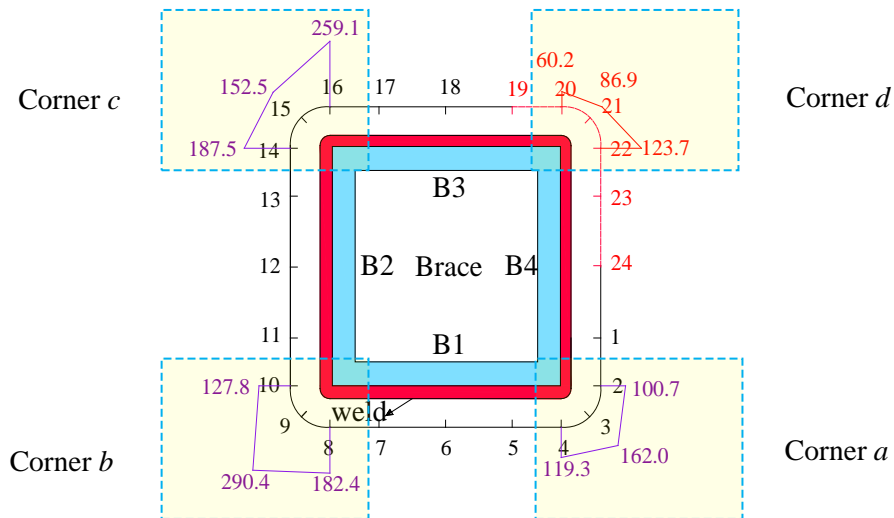


Fig. 19. Transverse residual stress distribution for the ambient temperature specimen at positions 20/25mm from the chord weld toe at the four corners.
(unit: MPa)

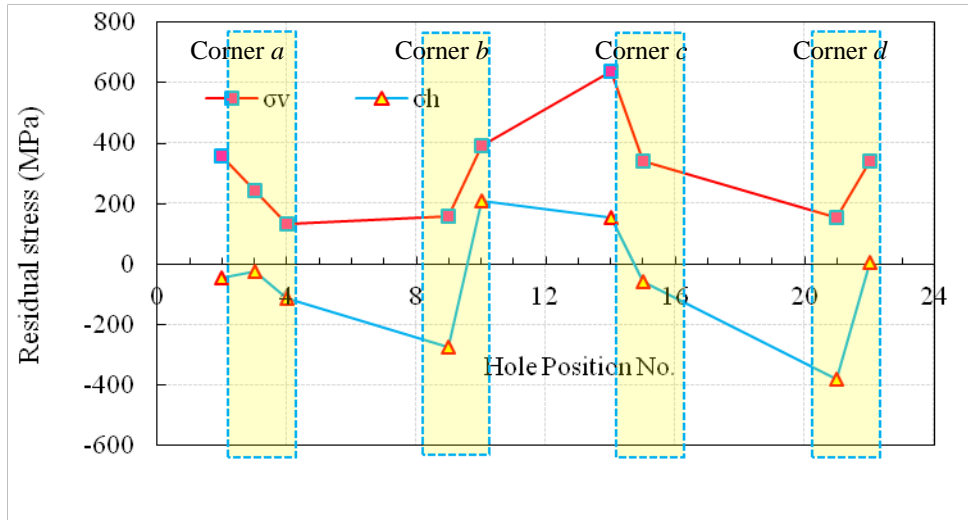


Fig. 20. Variations of transverse and longitudinal residual stresses at the chord weld toe estimated by linear interpolation for the ambient temperature specimen. (σ_v : transverse stress, σ_h : longitudinal stress)

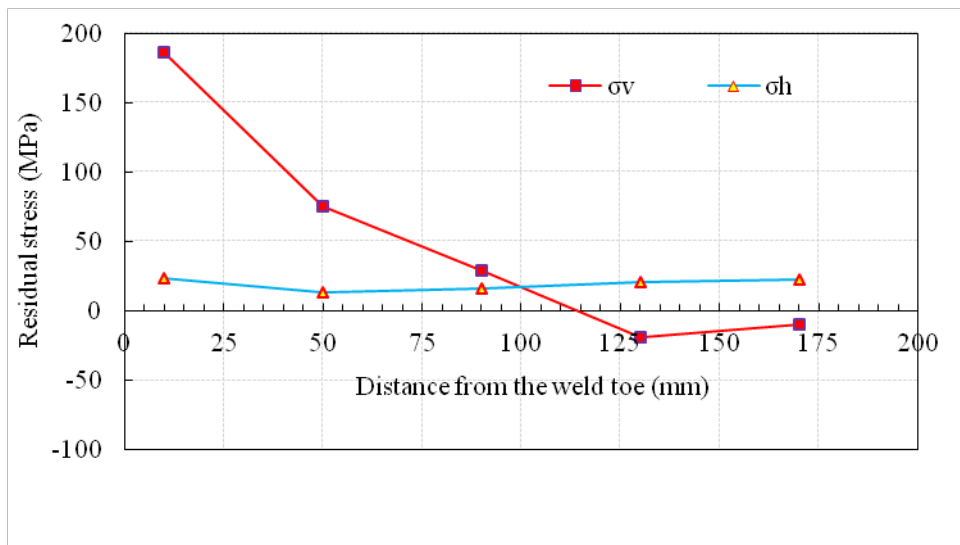


Fig. 21. Relationship between the transverse and longitudinal residual stress with distance from the weld toe for the ambient temperature specimen. (σ_v : transverse stress, σ_h : longitudinal stress)

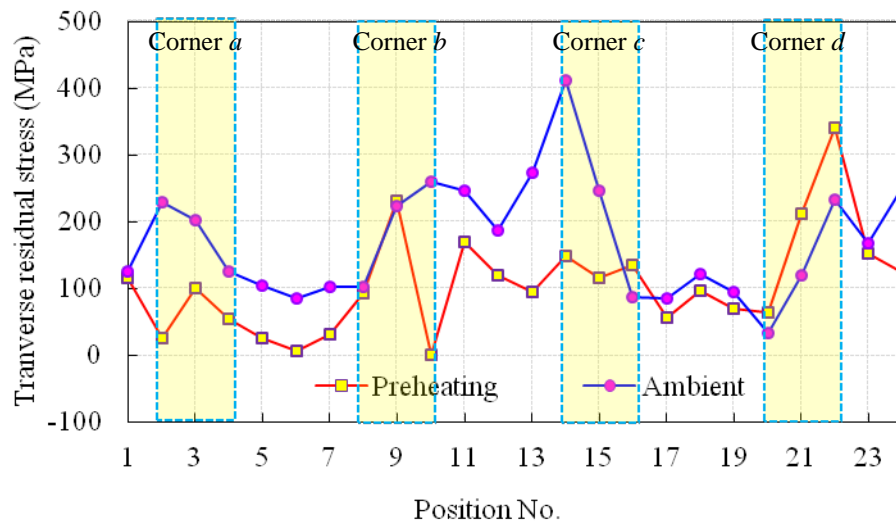


Fig. 22. Comparison of transverse residual stresses measured from two specimens.